Chapter 16

THE DERIVATION OF MERIDIONAL NEUTRAL WINDS IN THE THERMOSPHERE FROM F2-LAYER HEIGHT

K. L. Miller

Center for Atmospheric and Space Sciences
Utah State University
Logan, UT 84322-4405

P. G. Richards and D. G. Torr

Center for Space Plasma and Aeronomic Research
The University of Alabama in Huntsville
Huntsville, AL 35899

ABSTRACT

The measurement of neutral air motions is an important part of the World Ionosphere-Thermosphere Study. This paper describes a recently developed method of deriving the meridional component of the horizontal neutral wind in the thermosphere. The method is based on the approximately linear relationship between the height of the ionospheric F2-layer peak and the strength of the meridional neutral wind. An ionospheric photochemical model is used to compute the parameters that describe this relationship. The neutral wind speed is derived from a measurement of the height of the F2-layer (h_{max}). The measurement of h_{max} can be made by incoherent scatter radar and ionogram inversion techniques, but is also derivable from parameters that are routinely scaled from ionograms and archived in world data centers. The wind speeds derived from h_{max} are compared with winds from Fabry-Perot interferometry and incoherent scatter radar, and with results of the NCAR Thermospheric General Circulation Model.

1. INTRODUCTION

The understanding of the coupling between the neutral winds of the thermosphere and the ionosphere is one of the goals of the WITS program. While the measurement of many of the properties of the ionosphere can be made reliably using radio propagation and radar techniques, the measurement of the properties of the neutral thermosphere is difficult at best.

A measurement of the neutral air motions is valuable in any study of ionosphere-thermosphere coupling. The neutral wind affects many of the observable quantities and physical processes of the ionosphere, including the density profile of the ionospheric F region, and the generation and maintenance of electric fields.

There have been several models developed to describe the photochemistry and dynamics of the thermosphere and ionosphere [Torr et al, 1988; Sojka, 1989]. The models are becoming more and more complex, and are to a great extent limited by the accuracies of input parameters such as reaction rates, collision cross-sections, and solar

flux. One of the major limitations, especially to the electron density profile, is the lack of knowledge of the meridional neutral wind.

This paper describes a method to derive the meridional component of the neutral wind in the thermosphere from existing ionosonde measurements. The method has been shown to derive winds with comparable accuracy to other techniques. It has the advantage of being able to derive winds at any local time, and at any of the midlatitude ionosonde sites. Winds can be derived retroactively, since data from many ionosondes are routinely archived at the world data centers.

2. DEPENDENCE OF THE *F2*-LAYER HEIGHT ON MERIDIONAL WIND SPEED

Because of the magnetic control of the processes that determine the *F2*-layer height, the most useful coordinate system is one that reflects the direction of the geomagnetic field. Hence the use of the words "north" and "northward" in this paper always refer to magnetic north, and "meridional" always refers to the magnetic meridian. The declination of the magnetic field is generally less than 20° throughout the mid-latitude region. The largest declinations at mid-latitudes occur in the South Indian Ocean.

The component of the neutral wind that is parallel to the geomagnetic field affects the profile shape and thus the concentration of the ionization at *F*-region heights through ion-neutral collisions [Rishbeth, 1972]. Since vertical neutral drifts are normally small, the dominant collisional forcing is from the magnetically north-south component of the horizontal wind. A pole-ward component of the horizontal neutral wind will have the effect of forcing ionization downward parallel to the magnetic field, while an equator-ward component will have the opposite effect.

The motion of the ions maintained by a meridional neutral wind is dependent on the dip angle, I, of the geomagnetic field. Under quasi-steady-state conditions, the contribution to the northward parallel ion velocity (V_I) from the magnetically-northward neutral wind component (U_N) is

$$V_I = U_N \cos(I) \tag{1}$$

The vertical component of the ion velocity (V_z) that is due to this effect is

$$V_z = -U_N \sin(I) \cos(I) \tag{2}$$

If there is no externally applied forcing of vertical motion, the shape of the *F2* layer is determined by production, loss, and diffusion. The motion of the ions that is induced through the motion of the neutral wind either adds to or subtracts from the diffusion velocity of the ions. The height of the maximum ion density, or balance height, is determined by the altitude where the influences of loss and diffusion are approximately equal. If a force with a component parallel to the magnetic field is applied by an external source such as neutral wind or electric fields, the peak electron density is displaced from the balance height.

The variation of sin(I)cos(I) with magnetic latitude is shown in Figure 1. The magnetic dip angle in this figure was computed using the IGRF magnetic field model [Peddie, 1982]. The calculation was done at 255° E longitude since this meridian in the IGRF model includes the geomagnetic pole. Figure 1 shows that the effectiveness of the neutral wind to affect the height of the F2 layer decreases significantly at high and low latitudes. It is most effective near 25° from the geomagnetic dip equator where the dip angle is 45°. It is, however, a significant factor in determining the vertical ion motions in the F region throughout the midlatitude region.

3. DEVELOPMENT OF THE "SERVO" MODEL

Rishbeth [1966] and Hanson and Patterson [1964] showed that if the external forcing from the neutral atmosphere is not too great, there is a linear relationship between the height of the layer (h_{max}) and the neutral wind speed. Rishbeth [1967] compared the behavior of the F2 region under the influence of a meridional neutral wind to a servo system, and developed the equations describing the rate of vertical movement of the layer and the equilibrium position of the peak. According to the servo model, an equatorward wind will force the ionization to higher altitudes. The raising of the layer increases the downward diffusion, which in turn opposes further upward motion of the layer. Similarly, a poleward wind will force the ionization to lower altitudes where the increased recombination rate opposes a further lowering of the layer maximum. Except for extreme wind speeds, and if electric fields are small, a linear relationship holds approximately between the neutral flow (U_N) and the resulting change in the height of the F-layer peak [Rishbeth and Barron, 1960; Hanson and Patterson, 1964; Rishbeth, 1966; Buonsanto, et al. 1989].

By assuming an F2 region composed primarily of O^+ with an ionization peak well above the production region and a loss process dominated by the reaction of O^+ with N_2, Rishbeth et al. [1978] showed that an externally induced vertical drift and the rate of change of the layer height are related approximately by

$$\frac{dh_m}{dt} = \frac{D_m \sin^2(I)}{2H}\{\exp[-k(h_m-h_o)/H]-\exp[(h_m-h_o)/H]\}+V_z \qquad (3)$$

where

D_m = diffusion coefficient for O^+

I = magnetic dip angle

h_m = height of the F2-layer peak (h_{max})

h_o = balance height

H = scale height of the neutral ionizable gas

kH = scale height of O^+, which controls diffusion
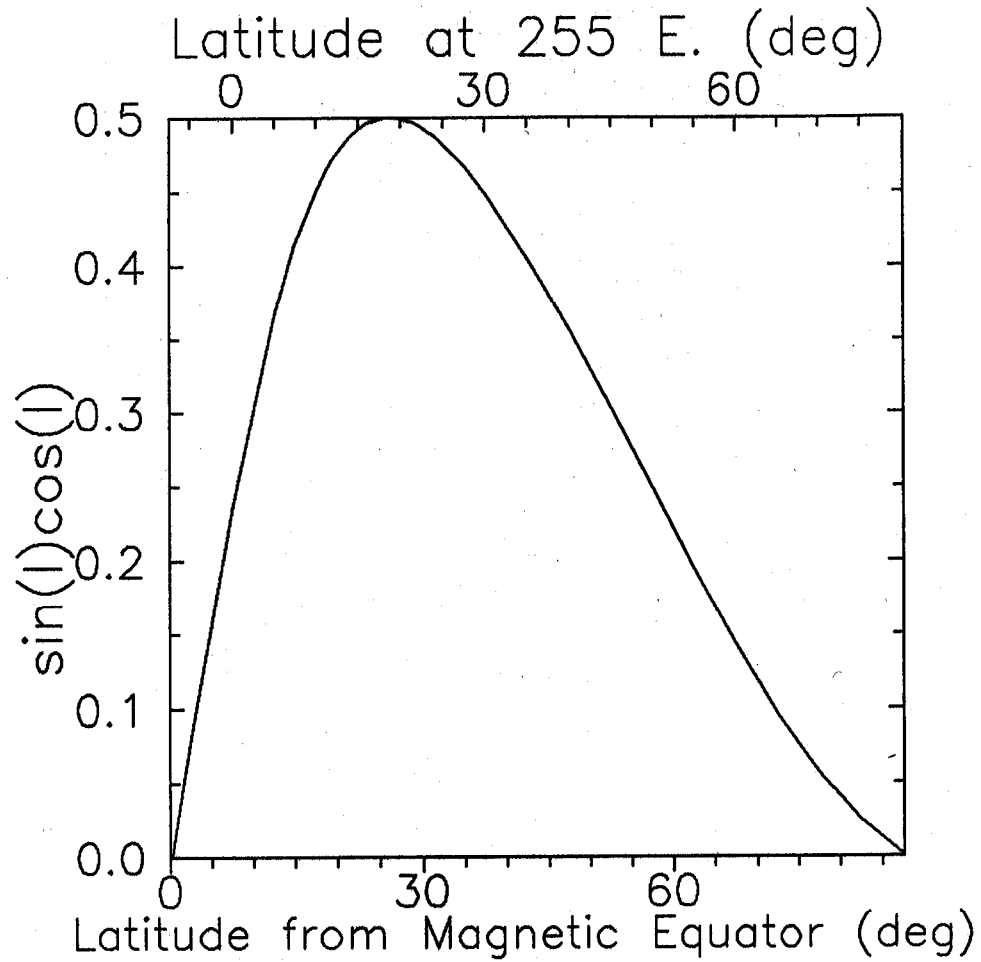
V_z = applied vertical ion drift

Figure 1. The ratio of vertical ion drift to horizontal neutral wind speed (sin(I) cos(I)) as a function of latitude north of the geomagnetic equator.

The plasma diffusion coefficient, D_m, is determined at the balance height, and is related approximately to the recombination coefficient at the peak, β_m, by

$$\beta_m = 0.628 \ \frac{D_m \ \sin^2(I)}{H^2} \tag{4}$$

in the daytime, and

$$\beta_m = 0.115 \ \frac{D_m \ \sin^2(I)}{H^2} \tag{5}$$

at night [Buonsanto, et al. 1989].

Equation 3 can be solved for the applied vertical drift, giving

$$V_z = \frac{dh_m}{dt} + \{\exp[(h_m\text{-}h_o)/H]\text{-}\exp[\text{-}k(h_m\text{-}h_o)/H]\}\frac{D_m \ \sin^2(I)}{2H} \tag{6}$$

Buonsanto et al. [1989] showed that, for most conditions in the F region, the effects of both the time rate of change of the layer height in the first term of Equation 6, and the non-linearity in the second term are small. Under these conditions, the vertical drift becomes

$$V_z = \frac{(k+1) \ D_m \ \sin^2(I)}{2H^2} (h_m\text{-}h_o) \tag{7}$$

If the vertical drift of the neutral atmosphere is assumed to be small, the vertical drift of the ionization can be assumed to be the result of a combination of ion collisions with the meridional component of the horizontal neutral wind and ion drift induced by the east-west electric field. Combining the E x B drift with Equation 2, the vertical drift can be written in terms of the northward neutral wind (U_N) and the eastward electric field (E_E) as

$$V_z = \text{-}U_N \ \sin(I) \ \cos(I) + \frac{E_E \ \cos(I)}{B} \tag{8}$$

For conditions existing most of the time at mid-latitudes, the "servo" equation yields meridional neutral wind speeds from measurements of the $F2$-layer height and a neutral atmosphere model using a simple relationship from Equations 7 and 8:

$$U_N = \frac{(h_0 - h_m)}{\alpha} + \frac{E_E}{B \ \sin(I)} \tag{9}$$

where

$$\alpha = \frac{2H^2 \ \cos(I)}{(k+1)D_m \ \sin(I)}$$

4. DEVELOPMENT OF THE "WIND FROM H_{MAX}" MODEL

Ionospheric models are dependent on winds and electric fields to define the profile shape and density of the F region. They contain within them the complex photochemistry that defines how h_{max} depends on the meridional wind speed. The models use this information in computing species concentrations when the neutral wind is specified.

If the east-west electric field is small, or if the effects of the meridional neutral wind and electric field are to be considered together, Equation 9 becomes a simple proportionality between wind and layer height:

$$U_N = \frac{(h_o - h_m)}{\alpha} \qquad (10)$$

Miller et al. [1986] took advantage of the capability of the FLIP model [Richards and Torr, 1985, 1988; Young, et al., 1980ab, Chandler et al., 1983] to compute h_{max} for a specified wind speed and developed a method to derive an approximate constant of proportionality for the relationship between $F2$-layer height and meridional wind speed.

4.1. Derivation of α and h_o.

A plot of h_{max} vs. meridional neutral wind speed has the characteristic "S"-shape shown in Figure 2. Figure 2 also shows the day to night difference in the response of h_{max}. The greater electron density in the daytime, combined with larger production and recombination rates result in a much stronger response of the layer height to small wind speeds, and then a much more rapid end to the linear portion of the curve. On the other hand, the nighttime change in layer height is smaller, with the linear region extending to greater equatorward wind speeds. The day-to-night difference in the response of the layer height to the neutral wind is important to the accuracy of wind speeds derived using this technique. The wind during the daytime is normally pole-ward and relatively small, while the nighttime wind is equator-ward and often near 200 m s^{-1}.

The form of Equation 10 suggests that in the linear region the neutral wind speed could be derived directly from measurements of the height of the $F2$-layer peak if α and h_o are known. These parameters can be derived using an ionosphere model to derive layer heights at several wind speeds, including h_o at $U_N = 0$, and then determining the slope (α) of the linear region. In practice, little accuracy is lost by finding h_{max} at two wind speeds that span the expected wind speeds but are still within the linear region, and then determining α from the slope of the line connecting the two points and h_o from the height where the line crosses $U_N = 0$.

4.2. Measurement of h_{max}

One of the advantages of having the capability to derive meridional wind speeds from h_{max} is the availability of data on a global scale from which h_{max} can be derived. The more traditional optical and incoherent scatter radar techniques of measuring neutral winds are valuable and provide checks on this method, but are limited in their coverage
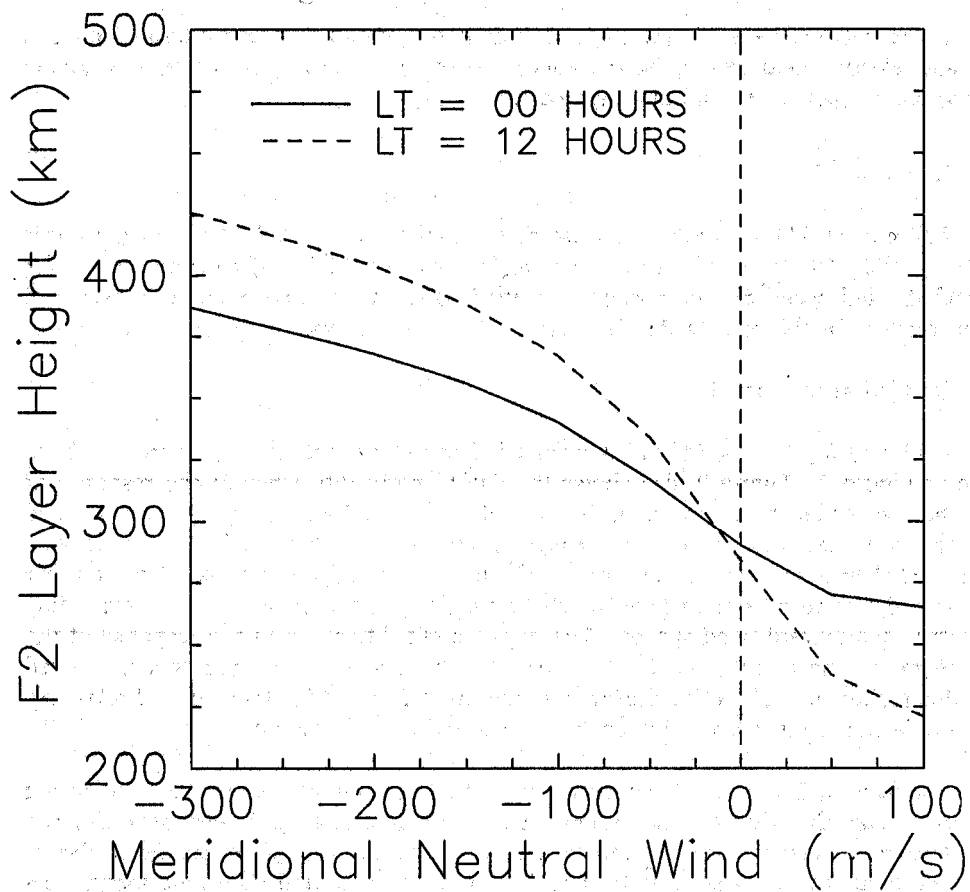
Figure 2. Height of the peak of the *F2* layer as a function of meridional wind speed at noon and midnight for equinox conditions.

by the weather and hours of darkness in the case of the optical measurements, and by the limited number and locations of the radars.

Ionosondes provide the data base from which global arrays of h_{max} can be derived. In simple terms, an ionosonde measures the time of flight of a radio pulse from the transmitter to the reflection point in the ionosphere and back to the ionosonde receiver. As the frequency increases, a virtual-height profile of the plasma frequency of the ionosphere, or ionogram, is generated. There is no reflection above the peak plasma frequency of the F2 region (foF2). To determine h_{max} the virtual height profile must be converted to a true height profile, or at least the true height of the reflection at foF2 must be determined.

In the best situation, the ionogram is either recorded digitally or hand scaled, and a true-height analysis converts the vertical heights of reflection to true heights [Titheridge, 1985]. It is tedious work to hand-scale a complete ionogram, and is not done routinely. Complete electron density profiles are being recorded, however, by a new generation of digital HF sounders.

At the present, any global study that relies on ionosonde data must derive its parameters from data that are routinely scaled from ionograms and archived in the World Data Centers. The parameters most relevant to this study are the maximum plasma frequency of the F2 region, foF2, the maximum frequency of the E region, foE, and the transmission factor M(3000)F2.

Dudeney [1983] reviewed the development of an empirical model that determines the layer height primarily from the approximately inverse relationship between the height of the peak of the F2 layer, hmF2 or h_{max}, and M(3000)F2. This model, based on work by Shimazaki [1955] and by Bradley and Dudeney [1973] uses M(3000)F2 for the primary calculation of F2 layer height, and uses the ratio of foF2 to foE as an indicator of the underlying ionization that retards the pulse and increases the virtual height. According to Dudeney [1983] the most accurate representation of the model is written as

$$h_{max} = \frac{1490 \ F}{M+\Delta M} - 176 \tag{11}$$

where

$$F=M \left(\frac{0.0196 \ M^2 \ + \ 1}{1.2967 \ M^2 \ - \ 1} \right)^{1/2}$$

$$\Delta M = \frac{0.253}{X_E - 1.215} - 0.012$$

$$X_E = \frac{foF2}{foE}$$

$$M = M(3000)F2$$

4.3. Accuracy of Derived Winds.

It is difficult to assign a realistic error bar to wind speeds derived from the *F2*-layer height. The major difficulty lies in the fact that it is based on an ionosphere model that predicts average behavior. Although the FLIP model generates the ionization density from photochemical reactions, it uses the MSIS empirical model for neutral densities and neutral temperature. The model performs well in tests against measurements [Chandler et al., 1983], but is unable to predict unusual or transient features.

A statistical error of the uncertainty in U can be estimated from Equation 10:

$$\frac{\Delta U}{U} = \left[\left(\frac{\Delta h_m}{h_o - h_m} \right)^2 + \left(\frac{\Delta h_o}{h_o - h_m} \right)^2 + \left(\frac{\Delta \alpha}{\alpha} \right)^2 \right]^{1/2} \tag{12}$$

Determination of Δh_o and $\Delta \alpha$ are based on the accuracy of the FLIP model. The height of the *F2*-layer peak is determined by a parabolic fit to the three points that define the peak ion density in the model. The step size can be adjusted, but is nominally about 8 km in the region of interest. A larger source of uncertainty is the degree to which the model represents the real ionosphere.

The value of h_o is derived from the point where the slope between h_m values at two wind speeds intersects U=O:

$$h_o = \frac{U_2 h_1 - U_1 h_2}{U_2 - U_1} \tag{13}$$

where the subscripts designate the two height/wind pairs. Assuming $\Delta h_1 = \Delta h_2 = \Delta h$, the RMS error in h_o is

$$\Delta h_o = \frac{\Delta h (U_2^2 + U_1^2)^{1/2}}{U_2 - U_1} \tag{14}$$

α is determined by the slope of the line connecting the two points:

$$\alpha = \frac{h_2 - h_1}{U_2 - U_1} \tag{15}$$

so that

$$\Delta \alpha = \frac{\sqrt{2} \, \Delta h}{U_2 - U_1} \tag{16}$$

The other quantity in Equation 10, h_m is subject to errors based on the type of measurement, the method of derivation, and also the time of day. h_m can be measured by incoherent scatter radar. This has the potential of being the most accurate, although the accuracy depends on various radar parameters such as the pulse length, signal-to-noise ratio, the conversion between scattered power and electron density, and the method of interpolation used to determine the maximum in the ionization density.

The majority of the h_{max} measurements on the global scale are made by ionosondes. The newer ionosondes are able to record the ionogram digitally and convert it to an electron density profile using a true-height analysis such as POLAN [Titheridge et al., 1985]. The majority of the ionosondes are still scaled by hand. The level of effort required to analyze an ionogram using a true-height analysis for hand-scaled ionograms is so great as to be impractical except for special campaigns.

The best alternative to a true-height analysis is to use an empirical formula, such as Equation 11, that determines the layer height from $M(3000)F2$. There have been few studies published of the accuracy of the $M(3000)F2$ technique. Dudeney [1983] suggests that the accuracy in the derived h_m is about 5%.

Figure 3 shows the derived meridional wind at Tokyo on 18 September 1984, during the Equinox Transition Study. The error bars in Figure 3 are the statistical error bars computed using Equation 12. The error bars are small compared with the diurnal variation of the derived winds, and are of comparable size to the hourly variability on this particular day. The winds are derived from data taken on a magnetically quiet day, and would normally be much more variable.

The greater sources of uncertainty are not statistical, however, but are systematic and derive from the lack of knowledge of many of the physical processes involved. The model used, while it represents a detailed photochemical description of the thermosphere and ionosphere, is representative of average conditions. Recently Burnside et al. [1987] has shown evidence that the O-O$^+$ collision cross section should be increased by a factor of approximately 1.7 over the previously used value. An increase in collision cross section in the FLIP model has the effect of significantly reducing the magnitude of the derived winds. Unless otherwise stated, the model results illustrated in this paper were derived using the larger collision cross section.

The magnitude of the east-west electric field also introduces a systematic error into the derived winds (Equation 9). There is currently no electric field model that has been shown to be accurate on a global scale, although some have successfully reproduced local measurements. This is, however, not a serious limitation if the results of the wind derivation is used as input to an ionospheric model, since the sum of the forces due to the meridional neutral wind and the electric field is the quantity needed by most models.

4.4. Dependence of h_o and α on Latitude, A_p, and F10.7

The response of the height of the $F2$ layer to changes in the meridional neutral wind speed depends strongly on the inclination of the geomagnetic field and of the local atmospheric conditions. As discussed above, the main determining factors of the layer height are the component of the neutral wind that is parallel to the magnetic field, diffusion of the ions along the field, and recombination.

Figure 4 shows the local time variation of α and h_o at four different magnetic latitudes, as computed by the FLIP model. The calculations were done for magnetically
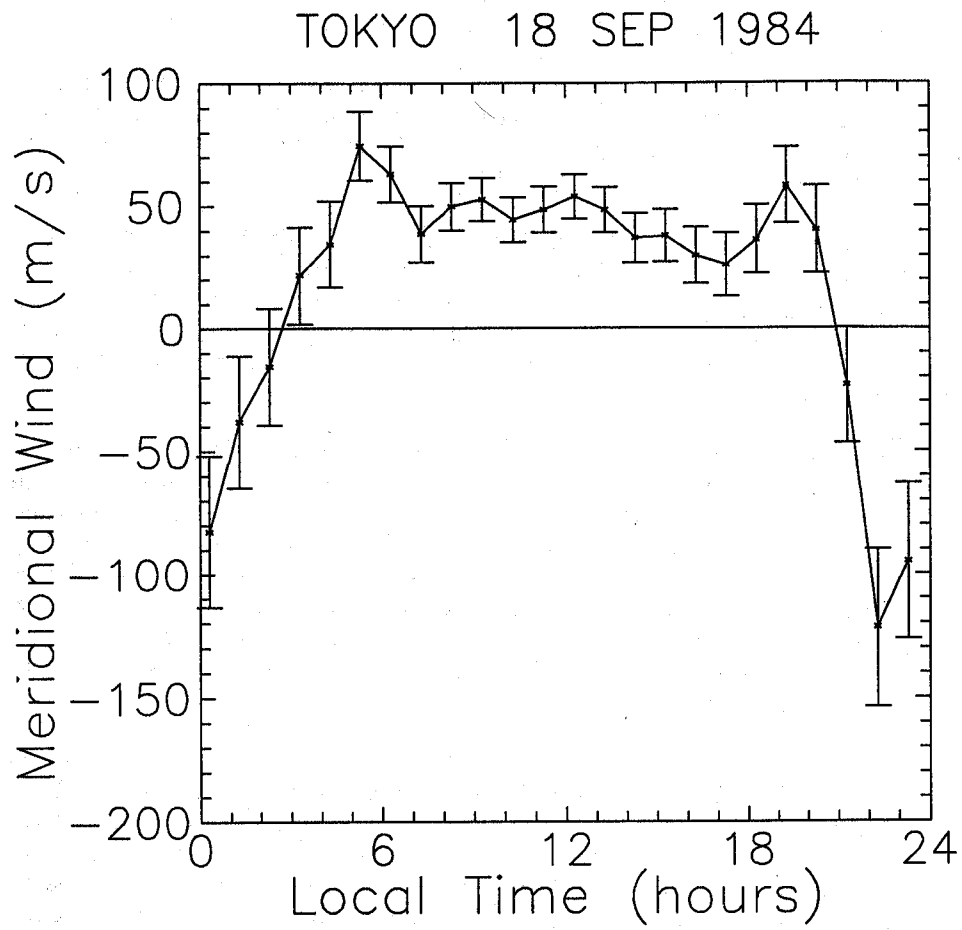
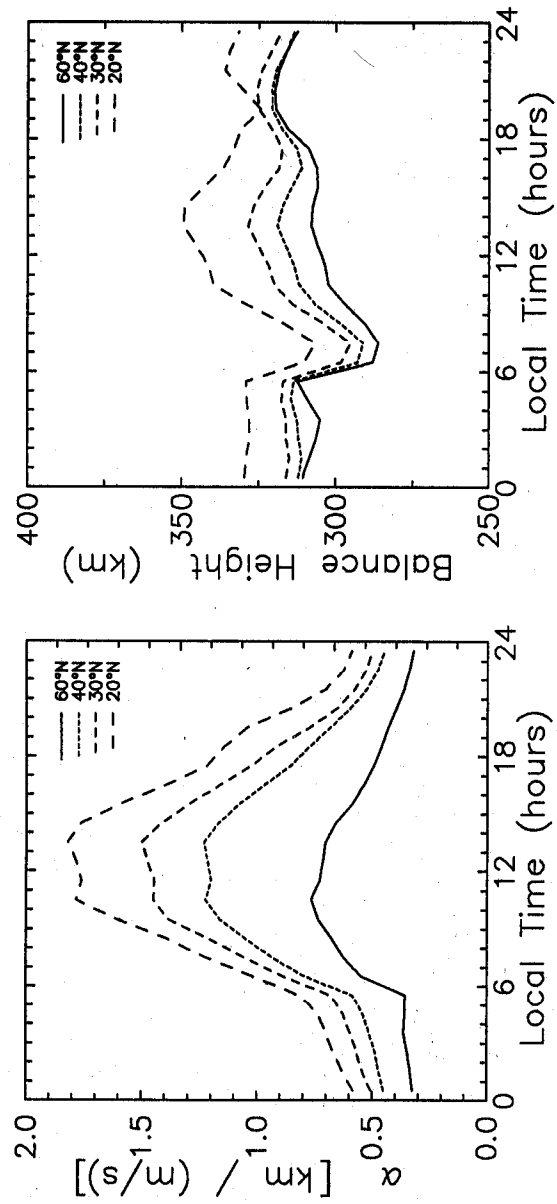Figure 3. Meridional wind speed at Tokyo (36° N, 140° E) on 18 September 1984. Error bars were computed using Equation 12.

Figure 4. Local time variation of α and h_o at four geomagnetic latitudes.

quiet conditions (A_p = 5) and moderate solar flux (F10.7 = 130) at a magnetic longitude of 0°.

A simple expression for the effect of latitude on α can be derived by assuming that the effect of a neutral component parallel to the magnetic field has a constant effect on the position of the peak of the layer along the field line at a given local time. In other words, at any given time,

$$\alpha_{||} = \Delta h_{||}/\Delta U_{||} \cong \text{constant,} \tag{17}$$

where the subscripts are to indicate that only the dimension parallel to the magnetic field is to be considered. The distance along the field line (h_2-h_1 in Equation 15) can be related to vertical distance by

$$\Delta h_m = \Delta h_{||} \sin(I) \tag{18}$$

and the component of the horizontal neutral wind along the field line to the horizontal wind by

$$\Delta U = \Delta U_{||} / \cos(I) \tag{19}$$

so that the value of α that relates vertical layer height to horizontal wind changes can be written in terms of $\alpha_{||}$:

$$\alpha = \alpha_{||} \sin(I) \cos(I) \tag{20}$$

This relationship was used by Forbes et al. [1988] to derive meridional wind speed from ionosonde data in a study of the penetration of auroral effects to low latitude during a magnetic storm. They fit the form of $\alpha_{||}$ published by Miller et al. [1986] to a mathematical function and scaled it by $\sin(I)\cos(I)$ to apply it to the latitudes of a meridional chain of ionosonde stations through Japan and the Soviet Union. Figure 5 shows $\alpha_{||}$ derived from the curves shown in Figure 4 using the dip angle from the tilted dipole magnetic field model used in the FLIP model. This seems to be a fair approximation at mid-latitudes, but departs from the calculated values at low latitudes.

Magnetic latitude is the primary geographic parameter in determining α and h_o. Even though the ionospheric density is affected by the neutral atmosphere, the effect of geographic latitude on the derivation of winds is much less important than the effect of magnetic latitude. Figure 6 shows the two parameters at four different longitudes, but all at a magnetic latitude of 40° North. Even though the geographic latitude varies from 29° to 51° North, there is very little difference in α or h_o.

Variation of α and h_o with respect to magnetic activity is shown in Figure 7. The calculations for Figure 7 and 8 are for 40° N, 0° E, magnetic coordinates. The variation is primarily in the balance height, although there is a small change in α. The insensitivity of these parameters to magnetic activity has important consequences in the study of storm effects, since they occur quickly and it is difficult to model the ionosphere with adequate time resolution.
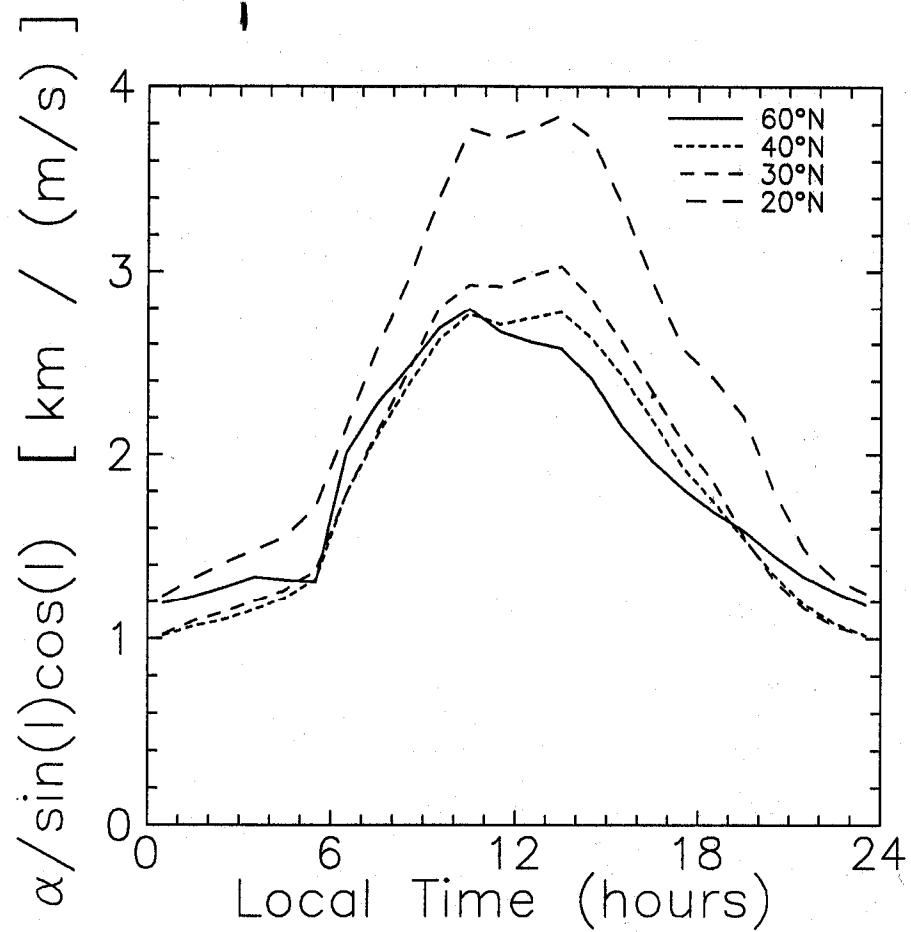
Figure 5. $\alpha_{\parallel}$ computed from values of α shown in Figure 4, and using the dip angle I from the tilted dipole magnetic field used in the FLIP model.
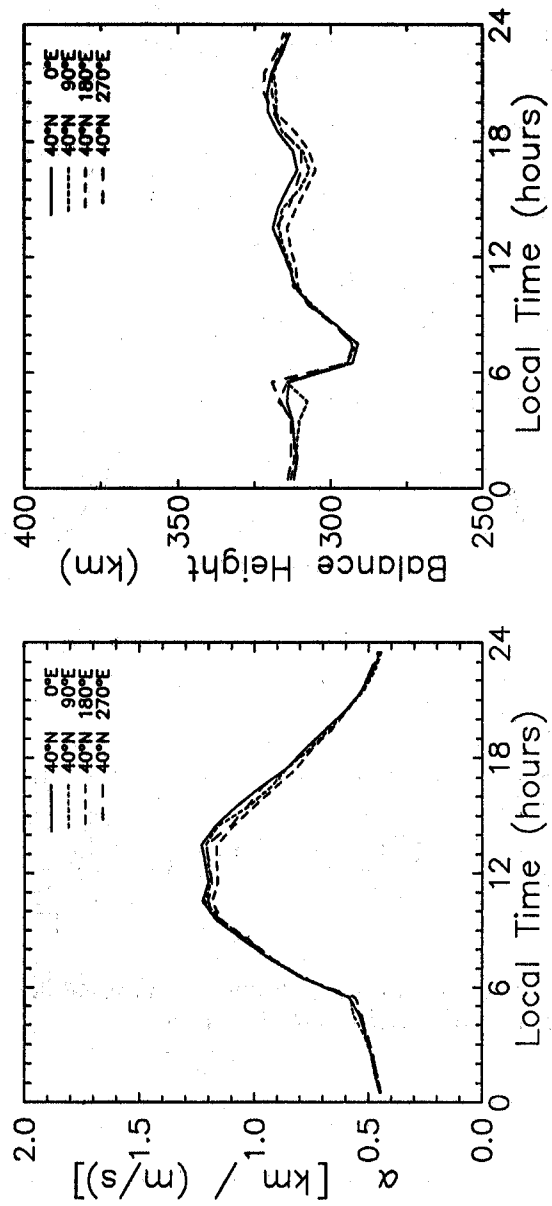
453

Figure 6. Local time variation of α and h_o at four geomagnetic longitudes. Magnetic latitude is 40° N.
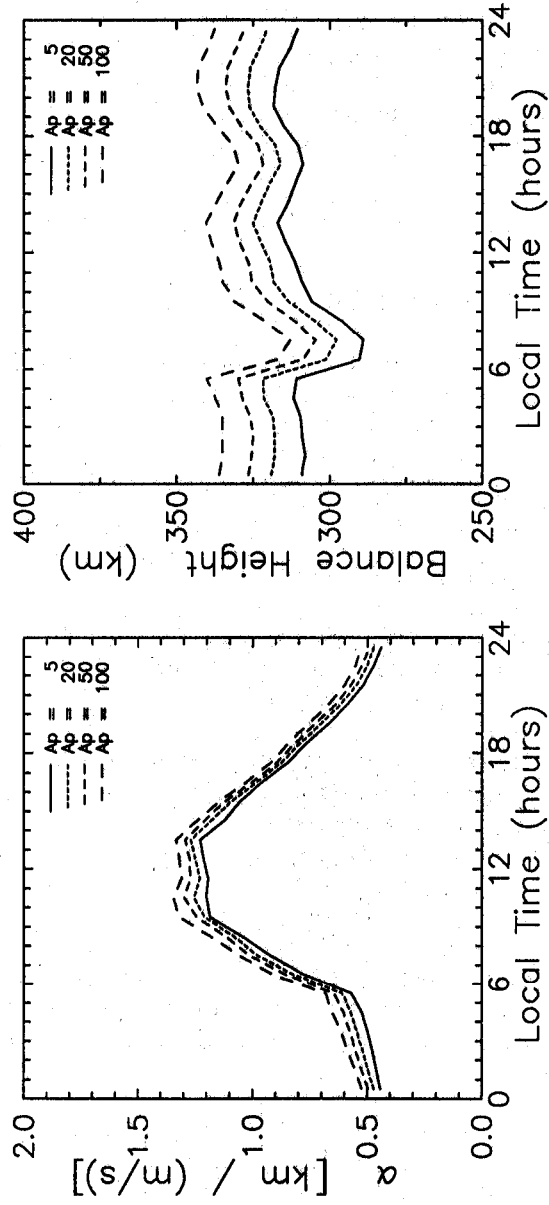
Figure 7. Local time variation of α and h_o with respect to magnetic activity.

A larger effect is found in the variation of α and h_o with changes in solar flux. Figure 8 shows α and h_o at low magnetic activity ($A_p = 5$) and at F10.7 values representative of conditions from solar minimum (F10.7 = 70) to solar maximum (F10.7 = 190). There are major differences in both α and h_o over this range of F10.7 values, mainly the result of the increased production rate of ionospheric O^+ and the larger scale height of the warmer neutral atmosphere at solar maximum. Although α and h_o are both strongly dependent on F10.7, it is such a slowly-varying function that it does not introduce a large uncertainty into the technique for deriving winds. While it will change significantly from month to month, there is very little day-to-day variation, even during magnetic storms.

5. CURRENT RESULTS

5.1 Comparisons With Other Wind Measurements

Several comparisons have been made of winds derived from h_{max} with meridional winds derived from other methods. These have been primarily with incoherent scatter radar, although Miller et al. [1986] also compared results with winds measured by Fabry-Perot interferometry. In each of these comparisons the wind speeds derived from h_{max} are consistent with the results of the other technique, both in the magnitude and in the pattern of variability of the winds.

Plots of the comparisons from Miller et al. [1986] are shown in Figure 9. The winds were measured at Arecibo using Fabry-Perot interferometry (F.P.I.) and derived from incoherent scatter ion drift measurements (v_b), and published by Burnside et al. [1983]. The curves labeled "Model" are derived from h_{max} without the 1.7 factor in the collision cross section [Burnside et al, 1987].

Miller et al. [1987] made a detailed comparison with the Millstone Hill incoherent scatter radar. This study had two objectives: First, to compare the difference between the results with the statistical uncertainty of the two derivations of wind speed. Second, to include measured electric fields in the calculation of winds from h_{max} to see if this would account for the difference.

The comparison was made for the Global Thermospheric Mapping Study (GTMS) campaigns of 26-18 June 1984 and 15-17 January 1985. Meridional neutral winds were derived from ion drift measurements for both campaigns. East-west electric fields were measured only during the June campaign. The factor of 1.7 was not used in the collision cross section in either wind derivation of this study.

Figure 10 shows the winds derived from h_{max} and from ion drifts for the two GTMS campaigns. The dashed curves are from incoherent scatter radar measurements of ion drift; the solid curves are derived from measurements of h_{max}. In this case, radar measurements of h_{max} were used. The results of the two derivations are quite similar, both in the magnitude of the wind and in the correlation of the features. An example is the abatement in the southward wind that occurs near sunset in January.
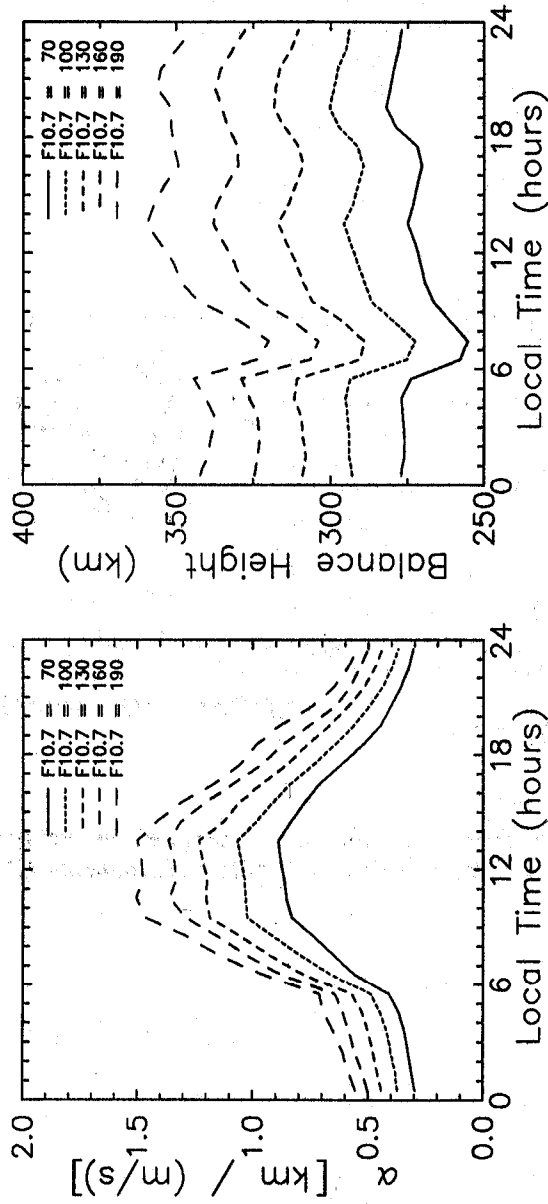
Figure 8. Local time variation of α and h_0 with respect to changes in solar flux. Range of F10.7 indices spans the expected difference from solar minimum to solar maximum.
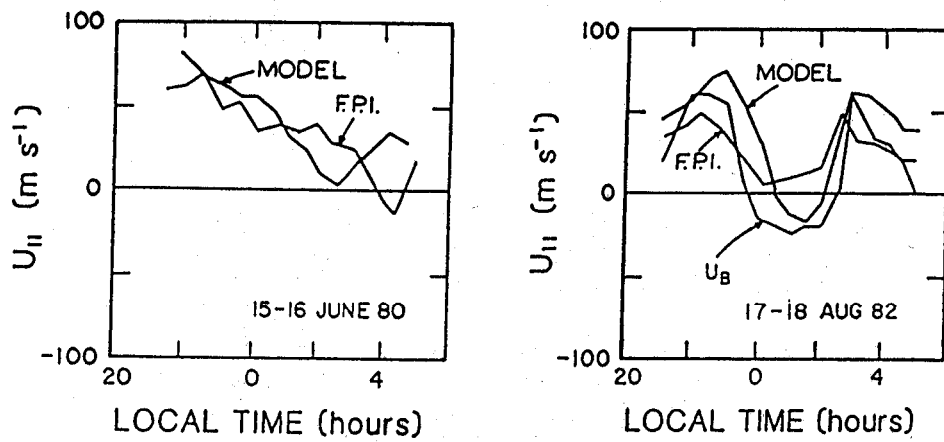
Figure 9. Comparisons of winds from h_{max} with winds measured by Fabry-Perot interferometry (F.P.I.) and by incoherent scatter ion drift measurements (U_B) for Arecibo [Miller, et al., 1986]
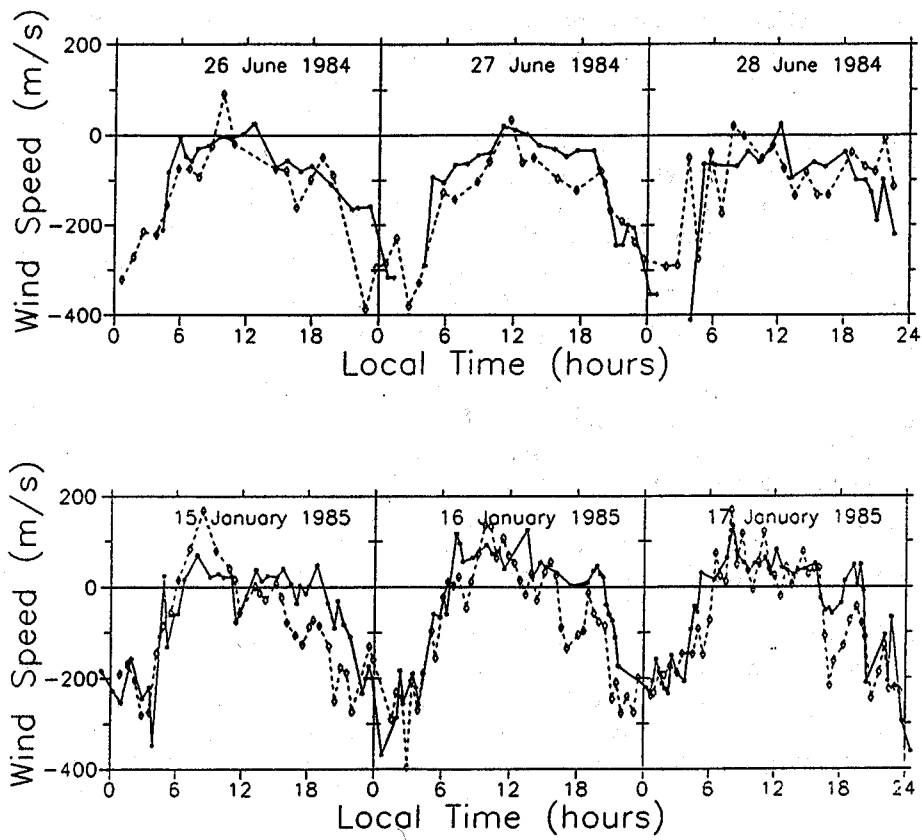
458

Figure 10. Comparisons of winds from h_{max} with winds derived from ion drift velocity measurements for 26-28 June 1984 and 15-17 January 1985. Dashed curves are from ion drift; solid curves are from h_{max}.

An attempt was made to determine the sources and magnitudes of the errors involved in these two derivations to see if the differences in the results are significant. The difference between the wind from h_{max} and the radar result was the greatest on 27 June 1984. The statistical error bars, shown in Figure 11, assume a 15-km uncertainty in the radar measurement of h_{max}. Figure 11 also shows the winds measured by the radar with their statistical error bars. With the exception of the afternoon near sunset the results are not significantly different. There are common sources of error inherent in both of these calculations. They both rely on model calculations, and are subject to the uncertainties inherent in models. An example is the uncertainty in the value of the O^+-O collision cross section.

Both the MSIS atmospheric model and the FLIP ionospheric model have been tested against many data sets, and have been shown to be reliable. However, a model, of necessity, must reflect average conditions. When daily departures of the models from actual conditions are considered, as well as uncertainties in the parameters used in the model calculations of both diffusion velocity and layer height, a more realistic error bar might be as large as 50 to 75 m/s. If 75 m/s error bars were used in Figure 11, the two wind curves would be within the error range of one another.

The east-west electric field was derived from ion velocity measurements made at Millstone Hill during the June campaign. The measured field, shown in Figure 12, was small throughout most of the time interval. The largest electric fields, reaching 4 mV/m in a westward direction, were measured on June 27.

Using Equation 9, we can determine the relative magnitude of the error introduced by neglecting the electric field. Figure 13 illustrated the results of including this measured field in the wind calculation. In Figure 13, the dashed curve is the wind from the incoherent scatter measurement. The solid curve was derived from h_{max}, and the dotted curve is the wind from h_{max} corrected by the electric field measurement, as described by Equation 9. On June 27, when the strongest electric fields were measured, the difference between the curves in the morning is accounted for by the 4 mV/m field. However, the measured electric field is not enough to reconcile the two wind curves in the afternoon.

Winds derived from ionosonde measurements cannot be independently verified. However, ionosondes near incoherent scatter radars should give similar results to the radars. An example is shown in Figure 14, where the meridional wind derived from ion drift measurements by the Millstone Hill radar are compared with the winds from h_{max} measurements by the Ottawa ionosonde for 26 June 1984. The two stations are separated by about 500 km in distance. Millstone Hill is at 42.5° N, 71.5° W, and Ottawa is at 45.1° N, 76.1° W.

The three-parameter formulation developed by Dudeney [1983] (Equation 11) was used to find the ionosonde values of h_{max}. There is agreement in both the wind speed and in the times of occurrence of the major variations at the two locations. The major feature is the abatement in the southward wind that occurs near sunset. This abatement was also seen in the wind values for the January GTMS period at Millstone Hill.
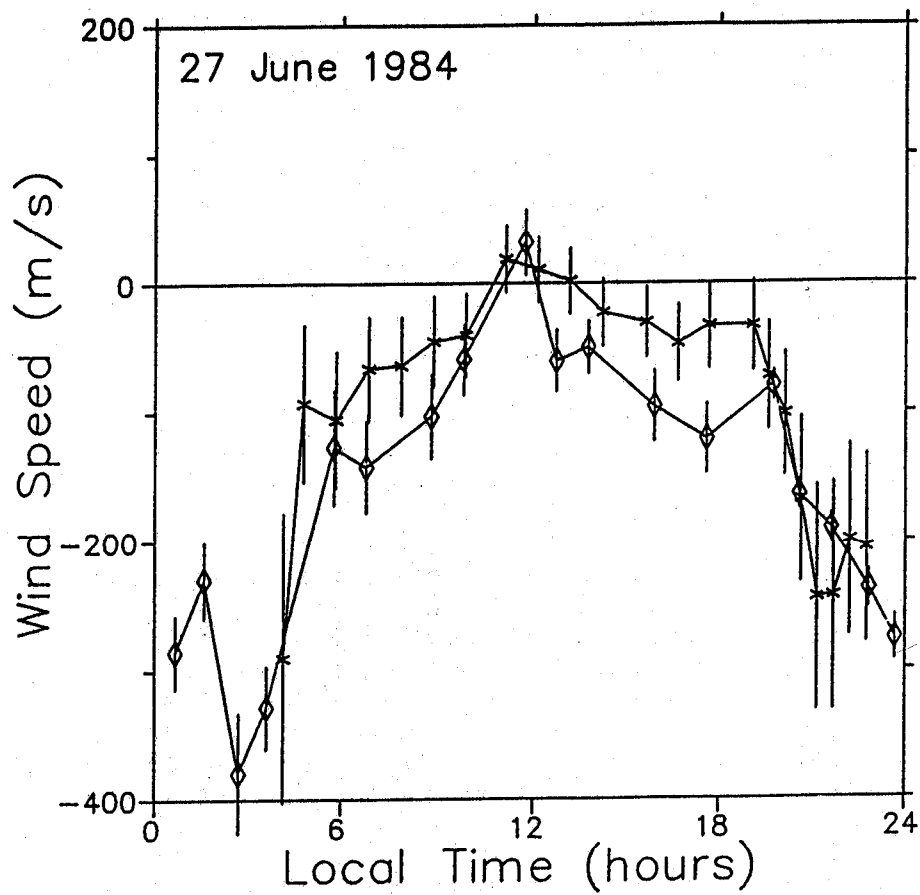
Figure 11. Meridional neutral wind speed at Millstone Hill, 27 June 1984, showing statistical uncertainty of the two derivations of wind speed. Diamonds show speed derived from ion drift measurements. Crosses are winds from h_{max}.
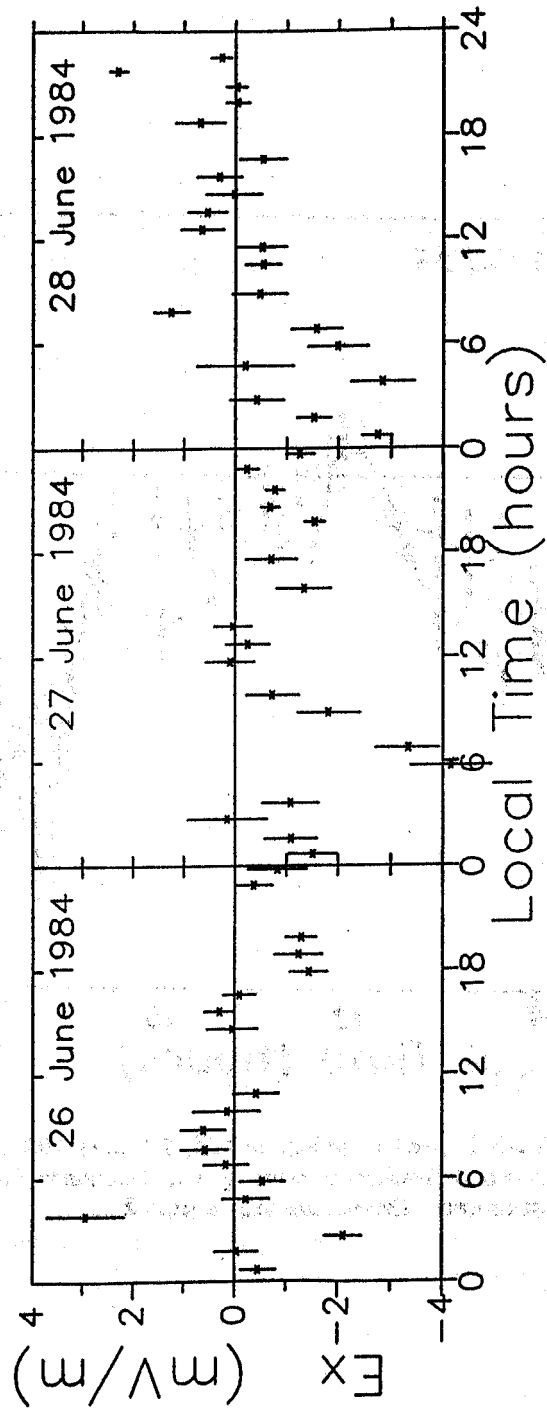
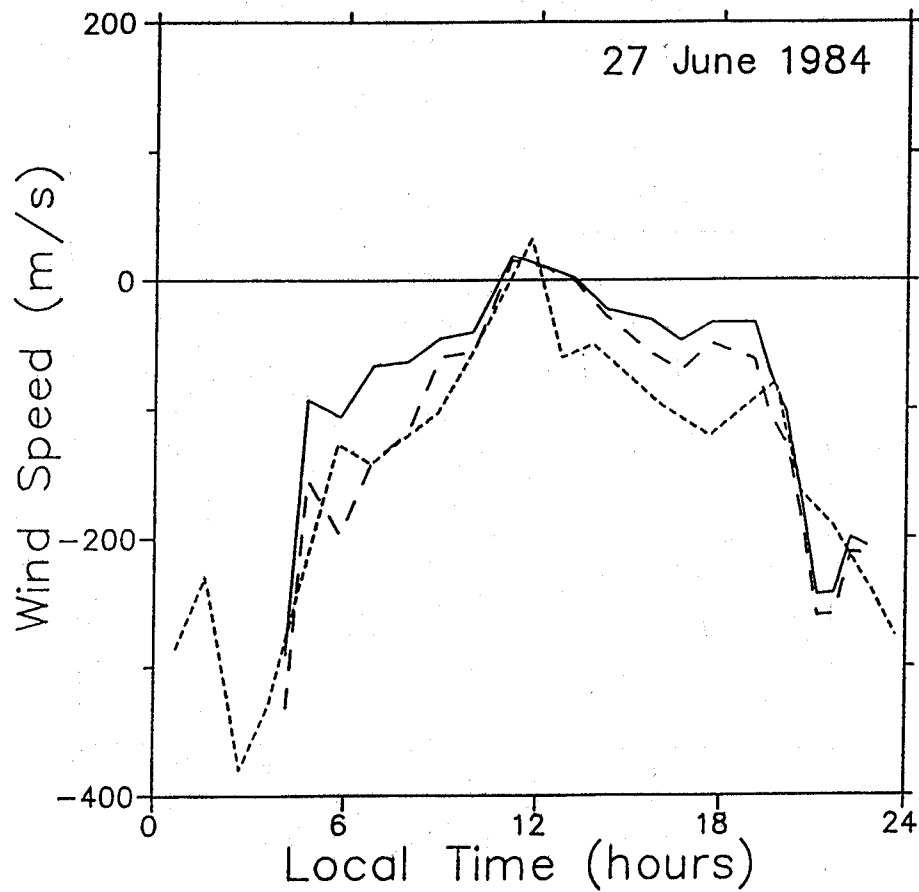Figure 12. Eastward electric field measured by the Millstone Hill Radar during the June, 1984, GTMS campaign.

Figure 13. Wind speed at Millstone Hill corrected for the effects of electric fields. The solid line shows wind speed from h_{max}; long dashes are wind from h_{max} with electric fields included; short dashes show wind speed from incoherent scatter ion drift measurements.
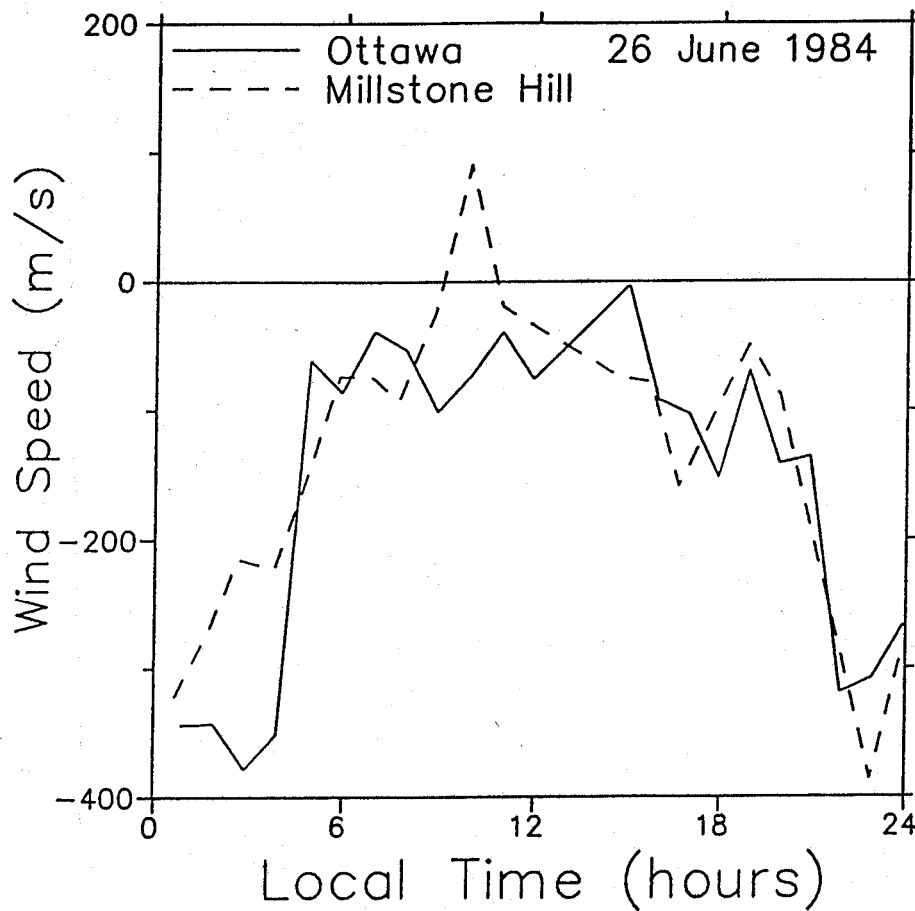
Figure 14. Meridional wind derived from ion drift measurements by the Millstone Hill Radar compared with the winds from h_{max} measurements by the Ottawa ionosonde for 26 June 1984. The two stations are separated by about 500 km in distance. Millstone Hill is at 42.5° N, 71.5° W, and Ottawa is at 45.1° N, 76.1° W.

A comparison of winds derived from h_{max} with results of the NCAR TGCM [Crowley, et al., 1989] is shown in Figure 15. This example is from the Equinox Transition Study of September 1984. Magnetic conditions were quiet on the first day, but the second day includes an equatorward surge at the onset of a magnetic storm. This was a "blind" comparison; no attempt was made to adjust either model to make it agree with the other.

5.2 Comparison With the Servo Model

In a recent study, Buonsanto et al. [1989] derived winds from an extensive Millstone Hill Radar data set using both the servo model and the FLIP model. The radar was being operated in a mode that used full north-to-south elevation scans for about seven days. The meridional neutral winds were derived from h_{max} from 30° to 55° latitude for seven days using both techniques. Although the derived winds are similar, servo-model winds are consistently more negative (stronger southward) than the winds derived using the FLIP model. The ratio of the two models is about 1.2 at night, and drops to near 0.5 in the daytime. Some of the difference may be due to the difference between the daytime and nighttime servo equations (see Equations 4 and 5), although a gradual transition is made between them. Another source of difference between the two techniques is the calculation of balance height. Also, in this case, the servo model used electron and ion temperatures that were derived from incoherent scatter radar measurements, while the FLIP model calculated the temperatures.

It would be convenient to be able to use a servo-type model to derive the wind values. However, the difference between the two techniques is significant. At this writing, an examination of the assumptions made in the two techniques and a comparison of them under a variety of conditions is being done to reconcile the results of the two techniques.

5.3 Support of Measurement Campaigns

Efforts to study ionosphere-thermosphere coupling are being coordinated through CEDAR on a national level, and through WITS and an international level. Both programs are interested in global wind values during campaigns. To date, the GTMS campaigns of June, 1984, and January, 1985; the ETS campaign of September, 1984; each of the GITCAD campaigns, and all but the first SUNDIAL campaign are supported by global-scale derivation of meridional wind speeds. Since the data required for the derivation of h_{max} are collected and archived routinely, it is possible to derive global scale meridional winds for any campaign.

5.4 Investigation of Solar Cycle Effects.

Breninger [1989], Miller et al. [1989], and Buonsanto [1990] have reported long-term trends in the meridional winds based on measurements of h_{max}. Breninger and Miller et al. examined data from several ionosondes over the last solar cycle and derived $hmF2$ values for the ten quietest days of January over an eleven-year period. Buonsanto used data from the ionosondes at Boulder and Wallops Island, and looked at diurnal, seasonal, and solar cycle variations. Each study reported a significant variation in the diurnal
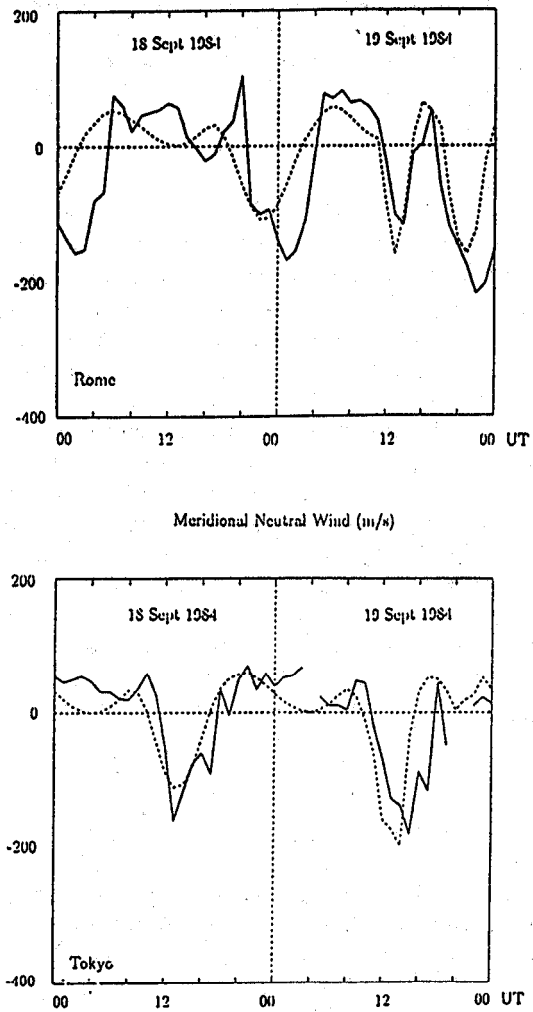
Figure 15. Meridional neutral winds measured (solid) and predicted (broken) for Rome and Tokyo. Negative values indicate equatorward winds; units are m s⁻¹ [Crowley et al., 1989].

amplitude of the wind variation at the northern (winter) hemisphere stations and attributed it to the increased ion drag on the neutral atmosphere at solar maximum. There is apparently a weaker variation, or at least a more confused situation, at low latitudes and in the southern (summer) hemisphere. In general, winds were strongest during solar minimum, but did not vary in the same pattern as the 10.7 cm flux or the sunspot number, as shown in Figure 16.

5.5 Development of a Global Wind Model.

As the reliability of the derivation of meridional neutral winds from ionosondes becomes established for quiet times, it will be possible to develop an empirical neutral wind model based entirely on ionosonde measurements. The size of the data base is already large enough to provide adequate diurnal and solar cycle coverage, although allowance must be made for the lack of coverage in some parts of the globe.

The possibility of a global wind model based on ionosonde measurements is illustrated by a study by Miller et al. [1990] to compare the winds derived from median ionosonde data for a 15-day period with winds derived from the International Reference Ionosphere (IRI) values of $hmF2$. Figure 17 shows agreement between ionosonde values and IRI values of the meridional wind speed at a set of ionosonde stations at approximately constant longitude. The stars show wind speed derived from 15-day median ionosonde measurements of h_{max}. The solid line is the wind speed derived from IRI values of $hmF2$. The dashed line that is included in Figure 17 is the wind speed from the HWM87 empirical wind model [Hedin et al, 1988]. The HWM87 model is based on a vector spherical harmonic fit to satellite wind measurements.

Comparing winds derived from ionosonde measurements with winds derived from the IRI is equivalent to comparing the IRI predictions of $hmF2$ with ionosonde measurement. However, it suggests the possibility of developing a global wind model based on the IRI. The reliability of such an empirical meridional wind model would be critically dependent on the reliability of the IRI values of $hmF2$. The IRI uses CCIR maps of ionosonde data to generate $hmF2$ values. These maps are, of course, most reliable in areas where the ionosonde measurements are most extensive, such as Europe and the Japanese-Australian meridian. To verify the accuracy of the IRI would be a long-term project, possibly using $hmF2$ and neutral wind measurements from satellites.
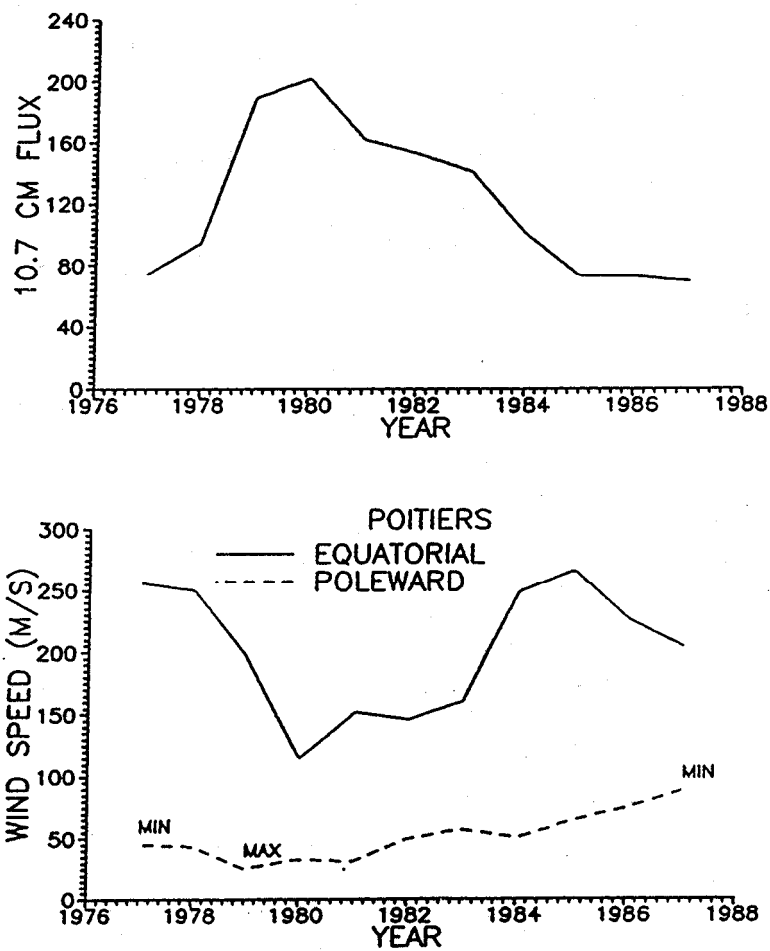
Figure 16. Variation of the equatorward (nighttime) and poleward (daytime) meridional winds for one solar cycle relative to the 10.7 cm solar radio flux. Units of flux are 10^{-22} W m^{-2} Hz^{-1} [Breninger, 1989].
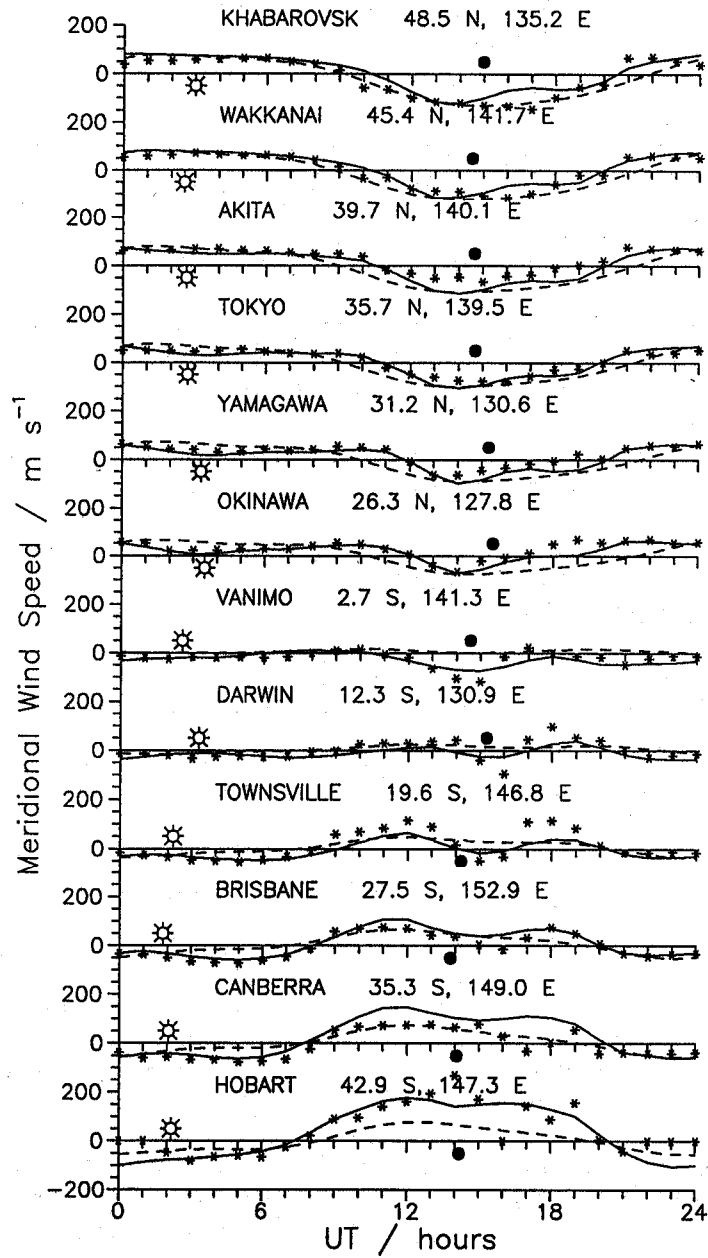
Figure 17. Meridional neutral wind speeds (m s⁻¹) at a meridional chain of ionosonde stations. Positive winds are northward. Stars are 15-day medians of ionosonde winds; solid line, IRI winds; and dashed line, HWM87 winds. Open and shaded circles mark local noon and midnight. [Miller, et al, 1990].

REFERENCES

Bradley, P. A., and J. R. Dudeney, A simple model of the vertical distribution of electron concentration in the ionosphere, J. Atmos. Terr. Phys., 35, 2131-2146, 1973.

Breninger, R. L., Solar cycle trend study of the mid-latitude quiet time meridional neutral winds at winter solstice conditions, M.S. Theses, Utah State University, 1989.

Buonsanto, M. J., J. E. Salah, K. L. Miller, W. L. Oliver, R.G. Burnside, and P. G. Richards, Observations of neutral circulation at mid-latitudes during the equinox transition study, J. Geophys. Res., 94, 16,987-16,997, 1989.

Buonsanto, M. J., Observed and calculated F2 peak heights and derived meridional winds at mid-latitudes over a full solar cycle, J. Atmos. Terr. Phys., in press, 1990.

Burnside, R. G., R. A. Behnke, and J. C. G. Walker, Meridional neutral winds in the thermosphere at Arecibo: Simultaneous incoherent scatter and airglow observations, J. Geophys. Res., 88, 3181-3189, 1983.

Burnside, R. G., C. A. Tepley, and V. B. Wickwar, The O^+-O collision cross-section: Can it be inferred from aeronomical measurements?, Annales Geophysicae, 5A, 343-350, 1987.

Chandler, M. O., R. A. Behnke, A. F. Nagy, E. G. Fontheim, P. G. Richards and D. G. Torr, Comparison of measured and calculated low-latitude ionospheric properties, J. Geophys. Res., 88, 9187-9196, 1983.

Crowley, G., B. A. Emery, R. G. Roble,, H. C. Carlson, Jr., J. E. Salah, V. B. Wickwar, K. L. Miller, W. L. Oliver, R. H. Burnside, and F. A. Marcos, Thermospheric dynamics during September 18-19, 1984. 1. Model simulations, J. Geophys. Res., 94, 16,925-16,944, December 1989.

Dudeney, J. R., The accuracy of simple methods for determining the height of the maximum electron concentration of the F2-layer from scaled ionospheric characteristics, J. Atmos. Terr. Phys., 45, 629-640, 1983.

Forbes, J. M., M. Codrescu and T.J. Hall, On the utilization of ionosonde data to analyze the latitudinal penetration of ionospheric storm effects, Geophys. Res. Lett., 15, 249-252, 1988.

Hanson, W. B., and T, N. Patterson, The maintenance of the night-time F-layer, Planet. Space Sci., 12, 979-997, 1964.

Hedin, A. E., N. W. Spencer, and T. L. Kileen, Empirical global model of upper thermosphere winds based on Atmosphere and Dynamics Explorer satellite data, J. Geophys. Res., 93, 9959-9978, 1988.

Miller, K. L., D. G. Torr, and P. G. Richards, Meridional winds in the thermosphere derived from measurement of F2 layer height, J. Geophys. Res., 91, 4531-4535, 1986.

Miller, K. L., J. E. Salah, and D. G. Torr, The effect of electric fields on measurements of meridional neutral winds in the thermosphere, Annales Geophysicae, 5A, 337-342, 1987.

Miller, K. L., R. L. Breninger, P. G. Richards, and D. G. Torr, The solar cycle variation of meridional neutral winds in the thermosphere, EOS, 70, 1243, 1989.

Miller, K. L., A. E. Hedin, P. J. Wilkinson, D. G. Torr, and P. G. Richards, Neutral winds derived from IRI parameters and from the HWM87 wind model for the SUNDIAL campaign of September, 1986, Adv. Space Res. 10, (8)99-(8)102, 1990.

Peddie, N. W., International Geomagnetic Reference Field: The third generation, J. Geomag. and Geoelec., 34, 309-326, 1982.

Richards P. G. and D. G. Torr, Seasonal, diurnal, and solar cycle variations of the limiting H^+ flux in the earth's topside ionosphere, J. Geophys. Res., 90, 5261-5268, 1985.

Richards, P. G. and D. G. Torr, Ratio of photoelectron to EUV ionization rates for aeronomic studies, J. Geophys. Res., 93 4060, 1988.

Rishbeth, H., and D. W. Barron, Equilibrium electron distributions in the ionospheric F2-layer, J. Atmos. Terr. Phys., 18, 234-252, 1960.

Rishbeth, H., F2-layer rates at sunspot minimum, J. Atmos. Terr. Phys., 28, 911-918, 1966.

Rishbeth, H., The effects of winds on the ionospheric F2-peak, J. Atmos. Terr. Phys., 29, 225-238, 1967.

Rishbeth, H., Thermospheric winds and the F-region: A review, J. Atmos. Terr. Phys., 34, 1-47, 1972.

Rishbeth, H., S. Ganguly, and J. C. G. Walker, Field-aligned and field-perpendicular velocities in the ionospheric F2-layer, J. Atmos. Terr. Phys., 40, 767-784, 1978.

Shimazaki, (1955), J. Radio Research Labs. Japan, 2, 85, 1955.

Sojka, J. J., Global scale, physical models of the F region ionosphere, Rev. Geophys, 27, 371-403, 1989.

Titheridge, J. E., Ionogram analysis with the generalized program POLAN, Report UAG-93, World Data Center A for Solar-Terrestrial Physics, NOAA, E/GC2, Boulder, CO, 80303, 1985.

Torr, D. G., P. G. Richards, and M. R. Torr, Photochemistry of the ionosphere, WITS Handbook, 1, 1-38, 1988.

Young, E. R., P. G. Richards, and D. G. Torr, A flux preserving method of coupling first and second order equations to simulate the flow of plasma between the photosphere and the ionosphere, J. Comp. Phys., 38, 141-155, 1980a.

Young E. R., D. G. Torr, P. Richards and A. F. Nagy, A computer simulation of the midlatitude plasmasphere and ionosphere, Planet. Space Sci., 28, 881, 1980b.